Probing the nature of electroweak symmetry breaking with Higgs boson pairs in ATLAS

Bartłomiej Żabiński
On behalf of the ATLAS Collaboration

35th Rencontres de Blois
October 20th-25th 2024

Higgs self coupling

Higgs potential:

$$V(\Phi)=\mu^2\Phi*\Phi+\lambda|\Phi*\Phi|$$

The λ can be measured directly in double Higgs boson production processes.

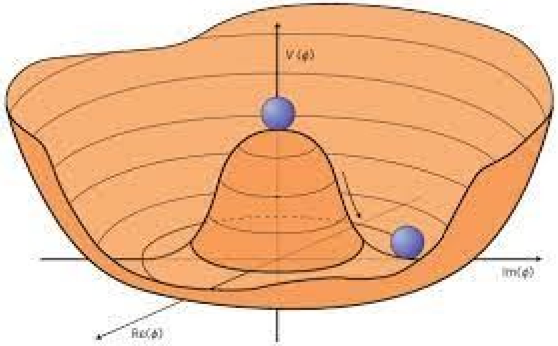

expanding around minimum:

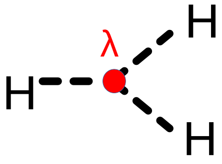

$$V(h)\simeq\frac{1}{2}m_H^2h^2+\lambda\upsilon h^3+\frac{1}{4}\lambda h^4+\ldots$$

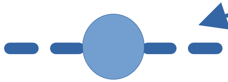

Probably beyond LHC - not enough data from LHC will be collected

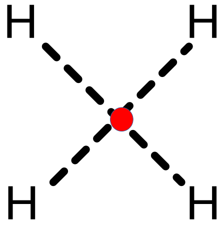

Double Higgs production

ggF: σ_{SM} ~ 31.5 fb

Coupling modifier $K_\lambda = \lambda/\lambda_{SM}$

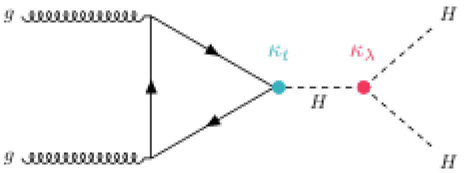

involves Higgs bosons self - coupling

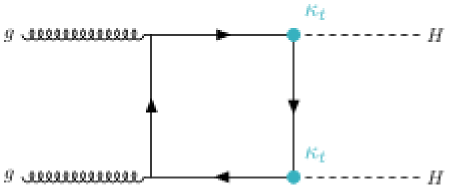

diagram interferes destructively

if K_λ > 1 could indicate processes beyond SM.

VBF: σ_{SM} ~ 1.72 fb

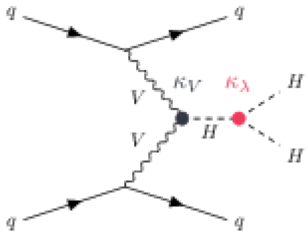

Sensitive for K_λ

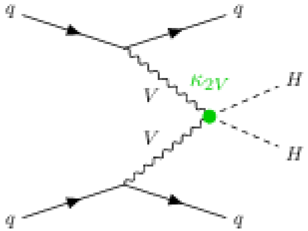

Access to HHVV coupling via K_{2V} coupling modifier

Two extra forward jets, unique signature

HH decay mode	bb	WW	ττ	ZZ	γγ
bb	33%				
WW	25%	4.6%			
ττ	7.4%	2.5%	0.39%		
ZZ	3.1%	1.2%	0.34%	0.076%	
γγ	0.26%	0.10%	0.029%	0.013%	0.0005%

Multiple diHiggs production channels:

- 4b – largest BR, huge background
- bbττ – small BR with relatively low background
- bbγγ – very small BR, but clean channel with low background,
- bbll – second largest BR
- ML – the combination of 9 channels with a small BR

The channels listed above will be discussed in this talk

Combination of the channels provides more precise results

Effective Field Theory (EFT)

Higgs EFT (HEFT)

► Describes Higgs bosons at low-energy dynamics without assumption of linear realization of EWSB

► The Higgs fields are treated independently

► Effective operators build from Higgs couplings

► Probe for anomalous Higgs behavior

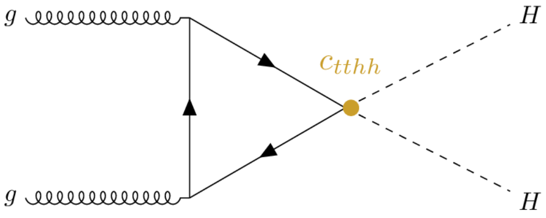

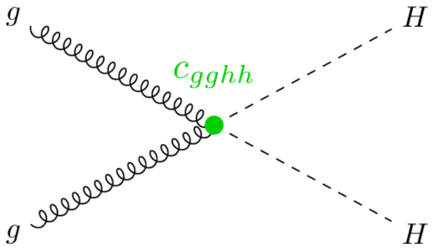

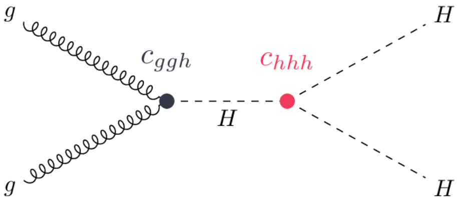

Wilson coefficients:
$C_{tth} \sim \kappa_t$, C_{tthh} , $C_{hhh} \sim \kappa_\lambda$, C_{ggh} , C_{gghh}

$$\mathscr{L}_{\mathrm{HEFT}} \supset -m_t \left(c_{tth}\frac{h}{v} + c_{tthh}\frac{h^2}{v^2} \right) \bar{t}t - c_{hhh}\frac{m_h^2}{2v}h^3 + \frac{\alpha_s}{8\pi}\left(c_{ggh}\frac{h}{v} + c_{gghh}\frac{h^2}{v^2} \right) G^a_{\mu\nu}G^{a,\mu\nu}.$$

HH → 4b

Event selection:

- 4 b-tagged jets
- Forward jets used to separate ggF and VBF regions
- Cut on HH and ttbar sensitive variables X_{HH} and X_{Wt}
- $|\Delta\eta_{HH}|$ and X_{HH} categories to improve κ_λ and κ_{2V} sensitivity

Analysis strategy:

- Jets paired to minimize ΔR for p_T leading dijet system
- Data from 2b region reweighed to 4b SR (data-driven bkg estimates)
- SR split into 6 ggF and 2 VBF categories
- m_{HH} distribution used to final results

$$R_{CR}=\sqrt{(m_{H1}-1.05\cdot 124\,GeV)^2+(m_{H2}-1.05\cdot 117\,GeV)^2}=45\,GeV$$

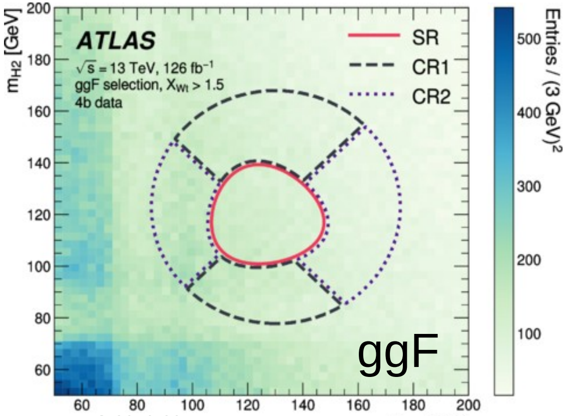

HDBS-2019-29

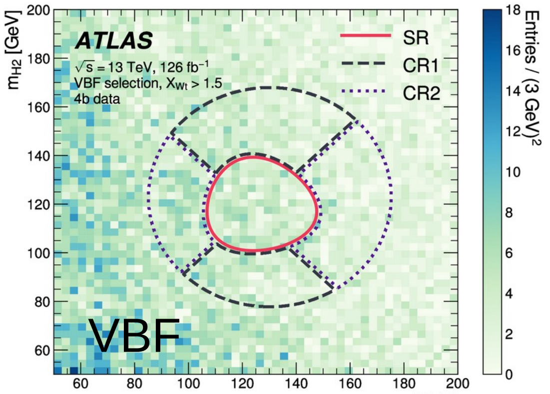

HDBS-2019-29

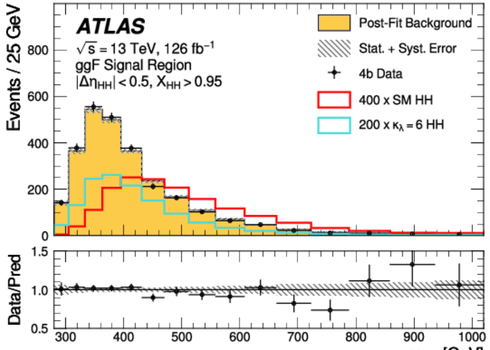

HDBS-2019-29

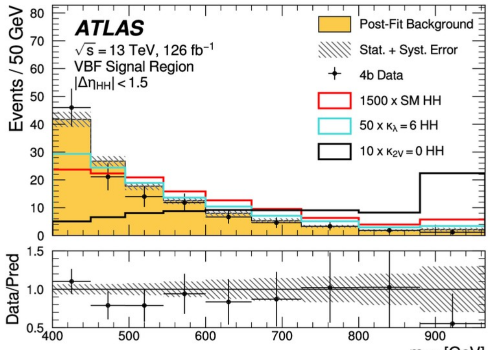

HDBS-2019-29

PHYSICAL REVIEW D 108, 052003 (2023)

HH → 4b

Results

μ_{HH} (Kλ=1,KV=1) < 5.4 σ_{SM} observed
8.1 σ_{SM} expected

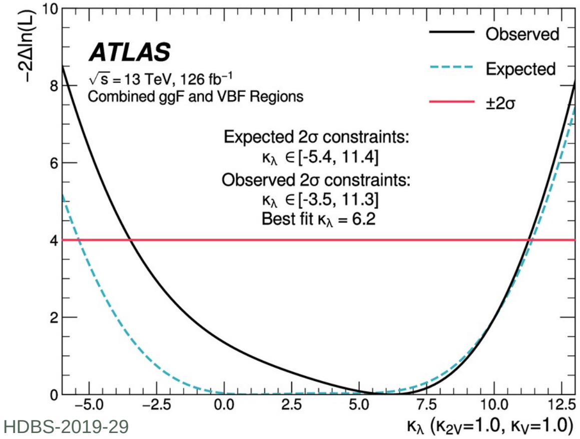

Observed: -3.5< K_{λ} < 11.3
Expected: -5.4< K_{λ} < 11.4

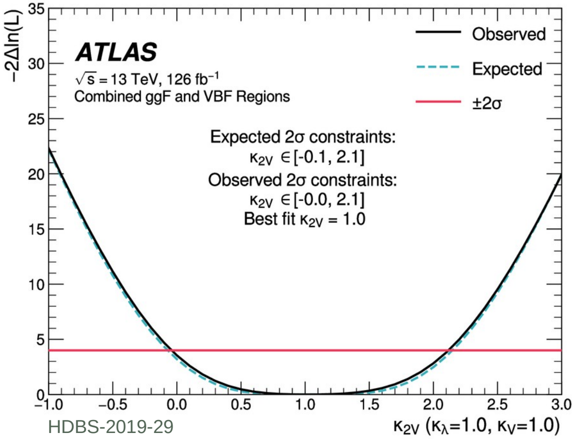

Observed: -0.0< K_{2V} < 2.1
Expected: -0.1< K_{2V} < 2.1

PHYSICAL REVIEW D 108, 052003 (2023)

HH → bbττ

Event selection:

- ♦ Exactly 2 b-tagged jets
- ♦ 1 hadronic τ and 1 e/μ or 2 hadronic τ
- ♦ $\tau_{had}\tau_{had}$ – pass single-$\tau_{had\text{-}vis}$ triggers STTs ,p_T > 100-180 GeV or Di-$\tau_{had\text{-}vis}$ triggers (DTTs) p_T > 40 (30)GeV
- ♦ $\tau_{lep}\tau_{had}$ - pass Single lepton triggers SLT or Lepton-plus-$\tau_{had\text{-}vis}$ (LTTs) p_T > 30 GeV
- ♦ $m_{\tau\tau}$ > 60 GeV using Missing Mass Calculator (arXiv:1802.08168v2)
- ♦ Signal region split into three categories - ggF Low-m_{HH} (m_{HH} < 350GeV) , ggF High-m_{HH}, and VBF
- ♦ Multivariate techniques (BDTs) were used to distinguish signal from background and used as the final signal/background discriminant.

$\tau_{had}\tau_{had}$

ggF Low-m_{HH}

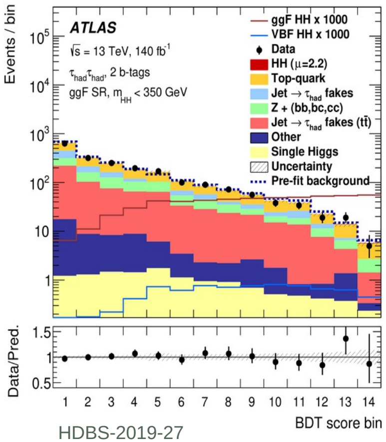

HDBS-2019-27

ggF High-m_{HH}

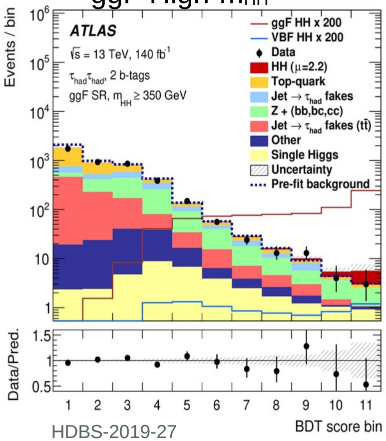

HDBS-2019-27

VBF

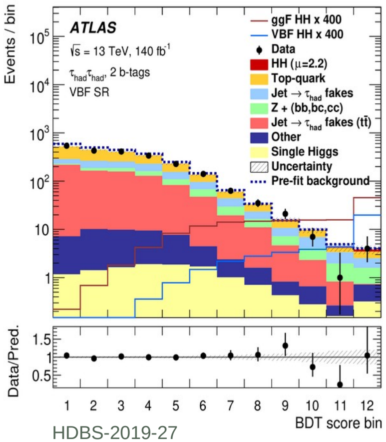

HDBS-2019-27

Multiple techniques for background estimation:

- MC shape and normalization from fit:
  # Top-quark processes
- MC shape and normalization from Z→μμ/ee+HF CR
  # Z→ττ + heavy flavor
- Data-driven method
  # Fake τ background
- Estimate from MC
  # Single Higgs and others

PHYS. REV. D 110, 032012 (2024)

Results

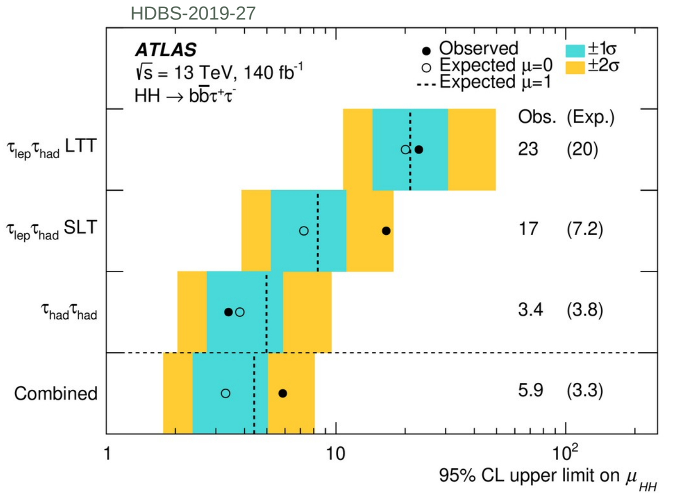

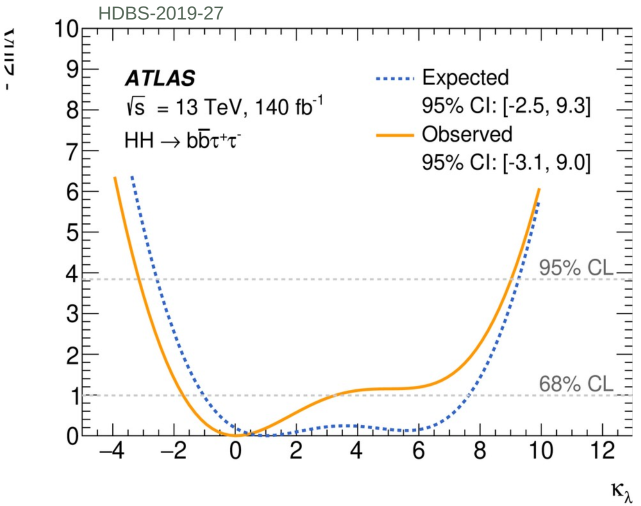

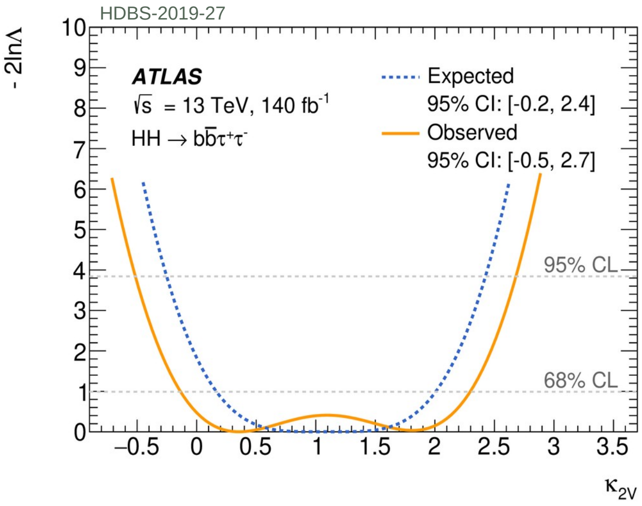

PHYS. REV. D 110, 032012 (2024)

μ_{HH} < 5.9 σ_{SM} observed
(3.3 σ_{SM} expected)

Observed: $-3.1 < K_\lambda < 9.0$
Expected: $-2.5 < K_\lambda < 9.3$

Observed: $-0.5 < K_{2V} < 2.7$
Expected: $-0.2 < K_{2V} < 2.4$

HH → bbγγ

Event selection:

- ➔ 2 photons with 105 GeV ≤ $m_{\gamma\gamma}$ ≤ 160 GeV
- ➔ The leading (subleading) photon p_T is larger than 35% (25%) of the mass of the diphoton system.
- ➔ Exactly 2 b-tagged jets
- ➔ No e/μ in event

* $m_{bb\gamma\gamma}$ distribution split to low masses (large k_λ, BSM) ,350 Gev boundry, and high masses (small k_λ, SM) regions
* combination of 2 BDT trainings to separate signal from single Higgs and continuum background

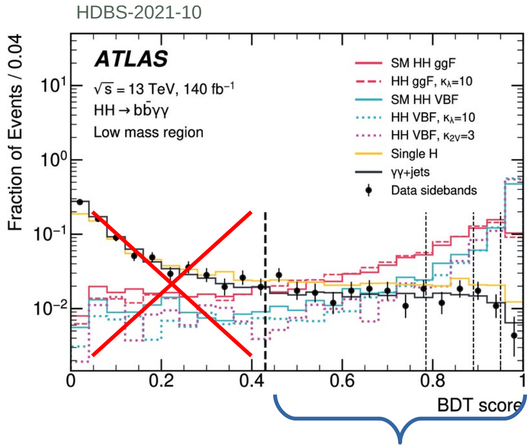

Divided into 4 categories

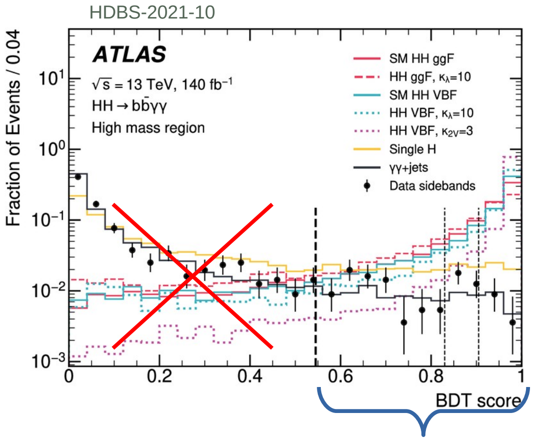

Divided into 3 categories

Signal extraction by fitting $m_{\gamma\gamma}$ distribution in each category and signal strength allowed to float

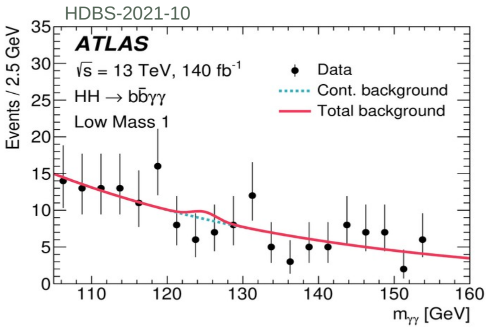

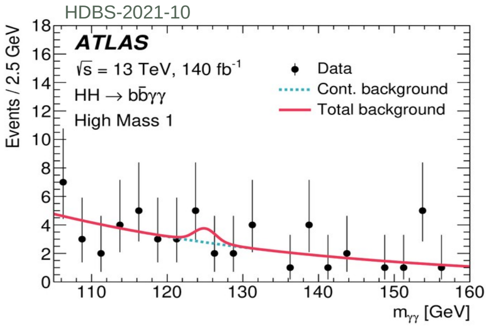

J. High Energ. Phys. 2024, 66 (2024)

HH → bbγγ

Results

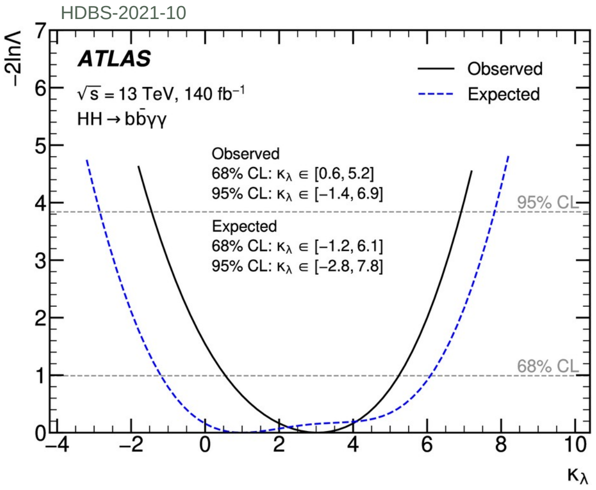

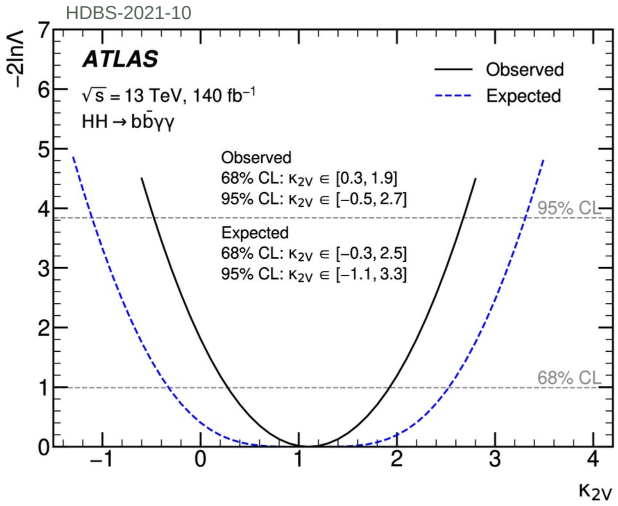

J. High Energ. Phys. 2024, 66 (2024)

μ_{HH} < 4.0 σ_{SM} observed
(5.0 σ_{SM} expected)

Observed: $-1.4 < K_{\lambda} < 6.9$
Expected: $-2.8 < K_{\lambda} < 7.8$

Observed: $-0.5 < K_{2V} < 2.7$
Expected: $-1.1 < K_{2V} < 3.3$

HH → bbll+ E_T^{miss}

Event selection:
- two light leptons (e,μ) with opposite charge
- two b-tagged jets with p_T> 20 GeV and |η| <2.5
- $m_{ll} \in$ SF (15, 75) GeV or DF (15,110) GeV

Signal region split into VBF and ggF sensitives regions
- VBF region - at least two forward jets with max|Δη| > 4, pT > 30 GeV, and max(mjj) > 600 GeV

To preselected events, DNN and BDT training were applied for ggF and VBF regions respectively.

HDBS-2019-02

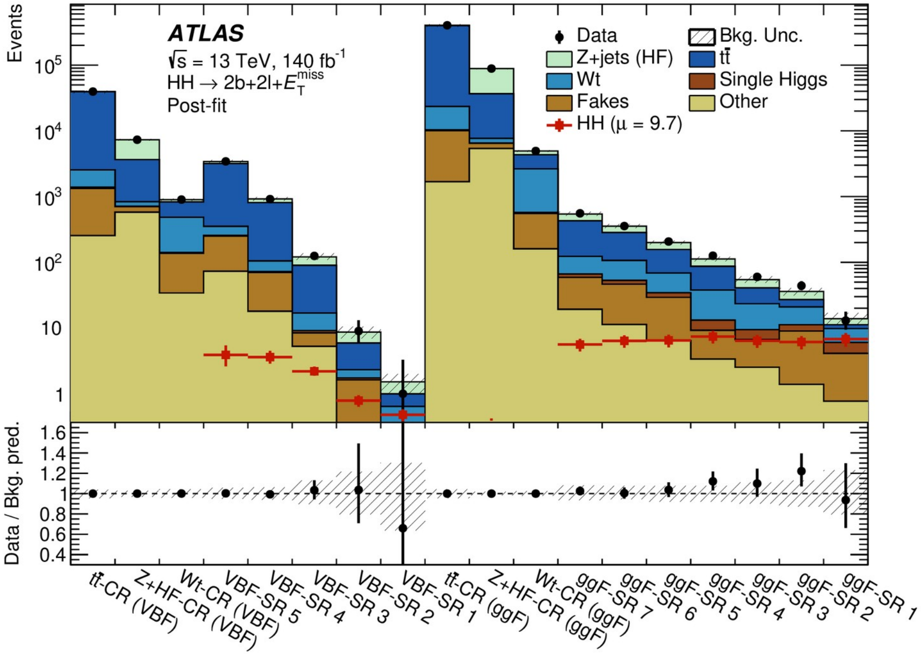

J. High Energ. Phys. 2024, 37 (2024)

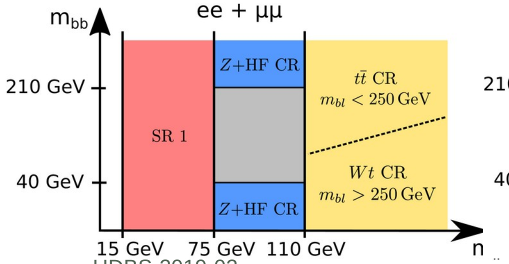

HDBS-2019-02

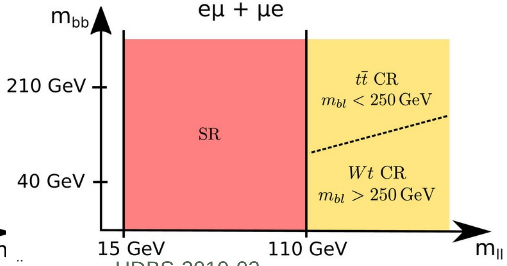

HDBS-2019-02

HH->bbll+ E_T^{miss}

Results

HDBS-2019-02

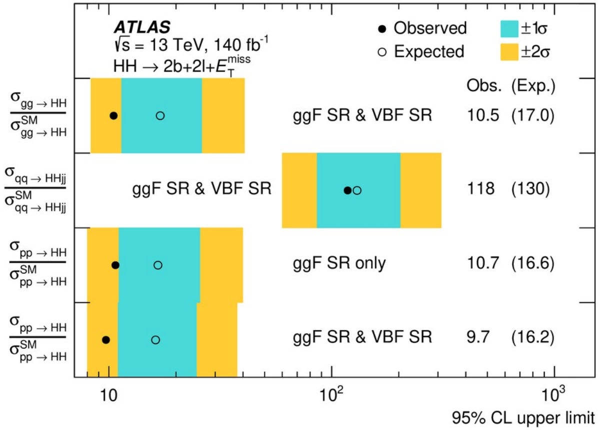

HDBS-2019-02

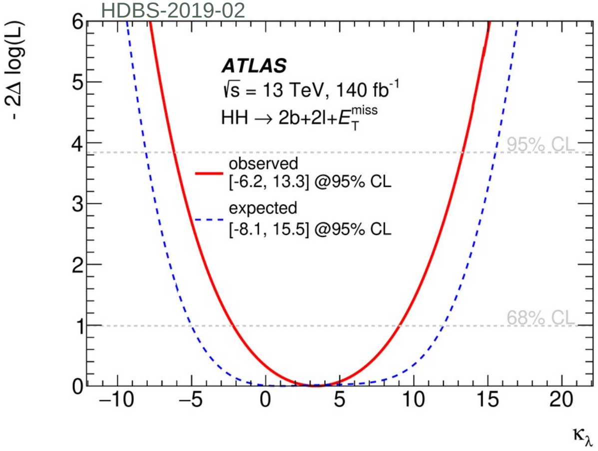

HDBS-2019-02

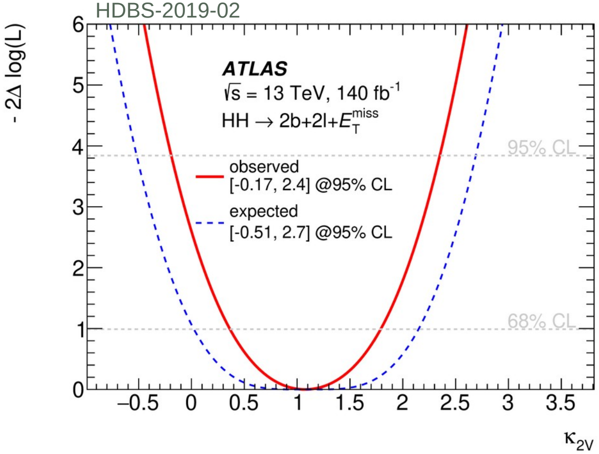

J. High Energ. Phys. 2024, 37 (2024)

μ_{HH} < 9.7 σ_{SM} observed
(16.2 σ_{SM} expected)

Observed: -6.2< K_λ < 13.3
Expected: -8.1< K_λ < 15.5

Observed: -0.17< K_{2V} < 2.4
Expected: -0.51< K_{2V} < 2.7

HH → ML

The analysis includes 9 channels with leptons in final state

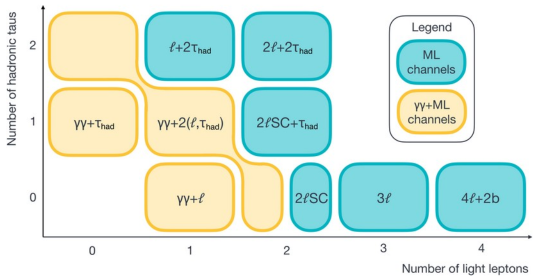

Multiple events selection concerning different channels.
All channels required no b-jets except 2b4l channel.

The BDT method is applied to preselected events to separate signal from background events.

The BDT score is divided into three regions in yy+ML channels.
The yy+ML channels use $m_{\gamma\gamma}$ distribution to obtain results.
Background modeling using sideband data

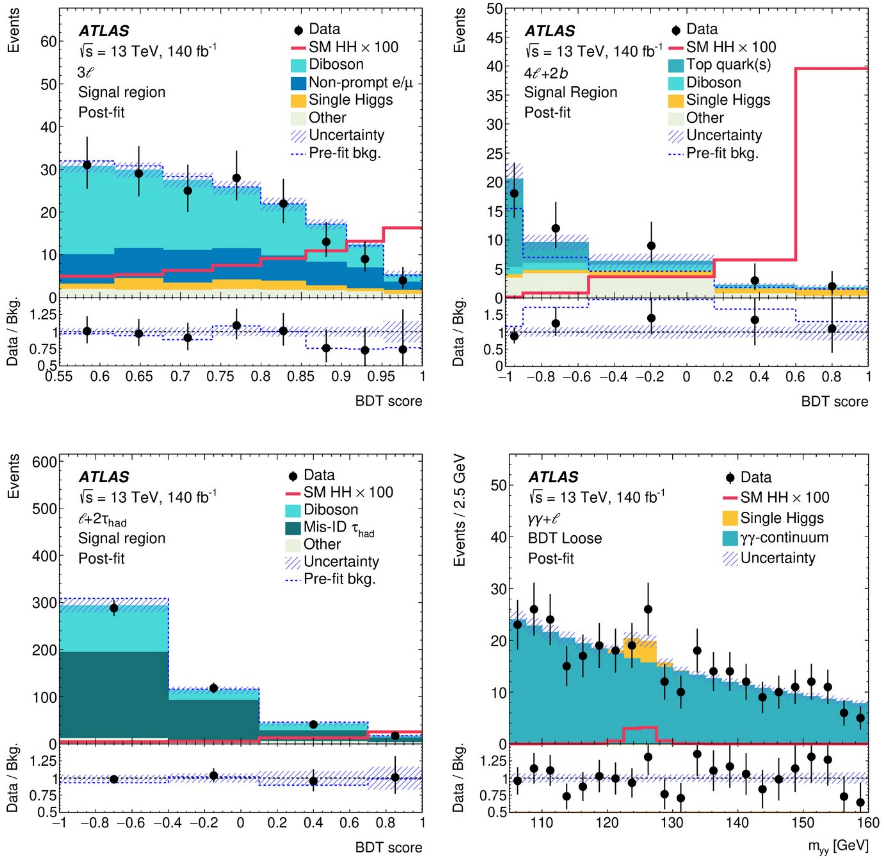

J. High Energ. Phys. 2024, 164 (2024)

HH → ML

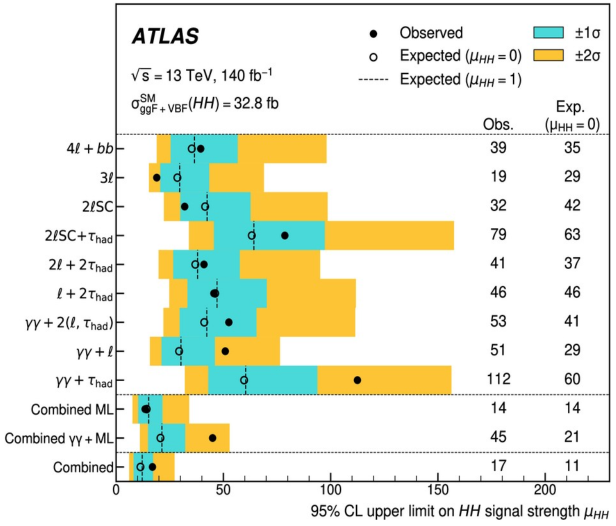

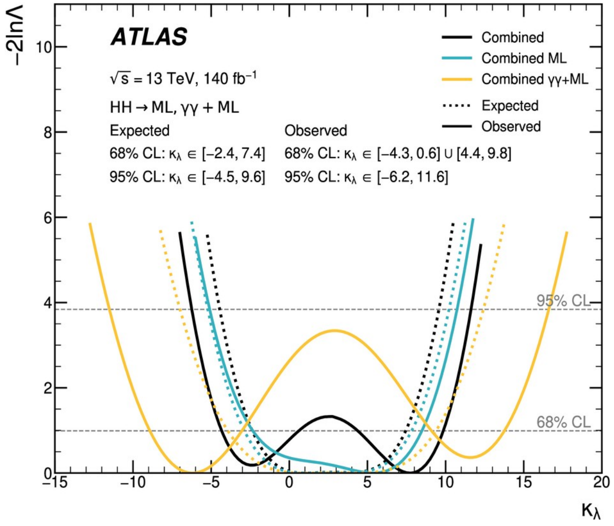

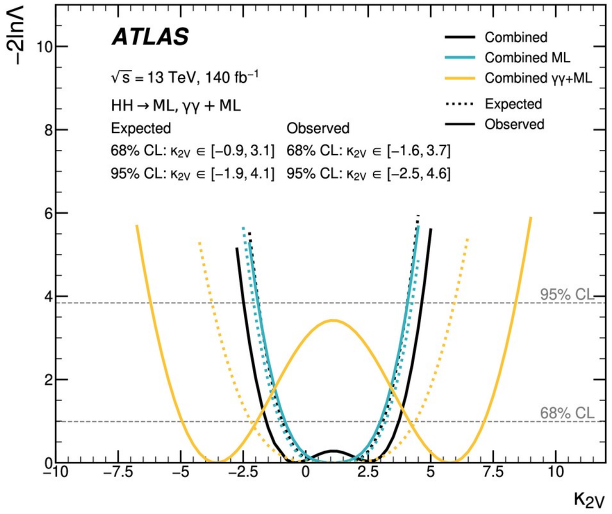

μ_{HH} < 17.0 σ_{SM} observed
(11.0 σ_{SM} expected)

Observed: -6.2< κ_λ < 11.6
Expected: -4.5< κ_λ < 9.6

Observed: -2.5< κ_{2V} < 4.6
Expected: -1.9< κ_{2V} < 4.1

J. High Energ. Phys. 2024, 164 (2024)

HH Combination

All presented channels have been combined.
Increased sensitivity by a statistical combination of HH channels

HDBS-2021-18

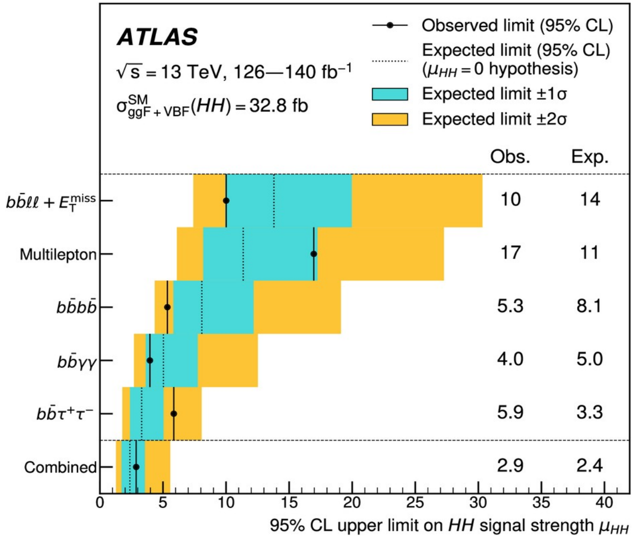

μ_{HH} < 2.9 σ_{SM} observed
(2.4 σ_{SM} expected)

HDBS-2021-18

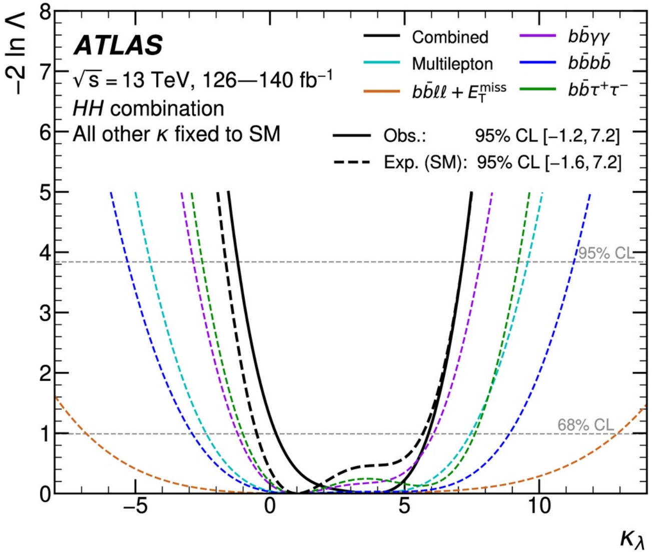

Observed: -1.2< K_λ < 7.2
Expected: -1.6< K_λ < 7.2

HDBS-2021-18

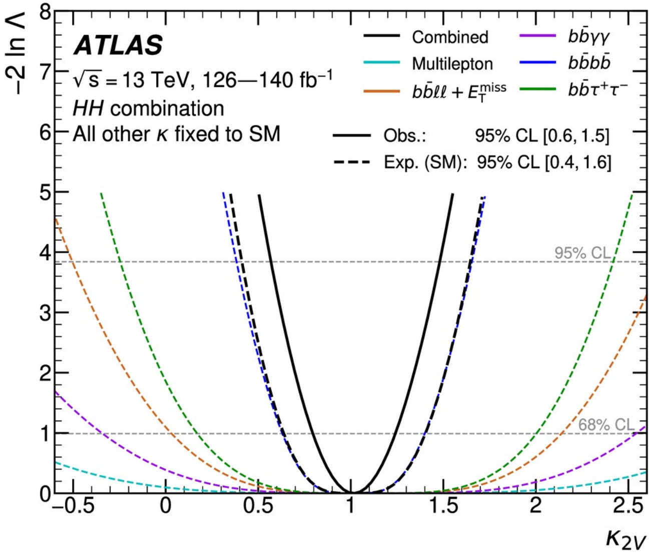

Observed: 0.6< K_{2V} < 1.5
Expected: 0.4< K_{2V} < 1.6

Phys. Rev. Lett. 133 (2024) 101801

HH Combination

Effective Filed Theory coefficient results

Benchmark Model	c_{HHH}	c_{ttH}	c_{ggH}	c_{ggHH}	c_{ttHH}
SM	1	1	0	0	0
BM1	3.94	0.94	1/2	1/3	−1/3
BM2	6.84	0.61	0.0	−1/3	1/3
BM3	2.21	1.05	1/2	1/2	−1/3
BM4	2.79	0.61	−1/2	1/6	1/3
BM5	3.95	1.17	1/6	−1/2	−1/3
BM6	5.68	0.83	−1/2	1/3	1/3
BM7	−0.10	0.94	1/6	−1/6	1

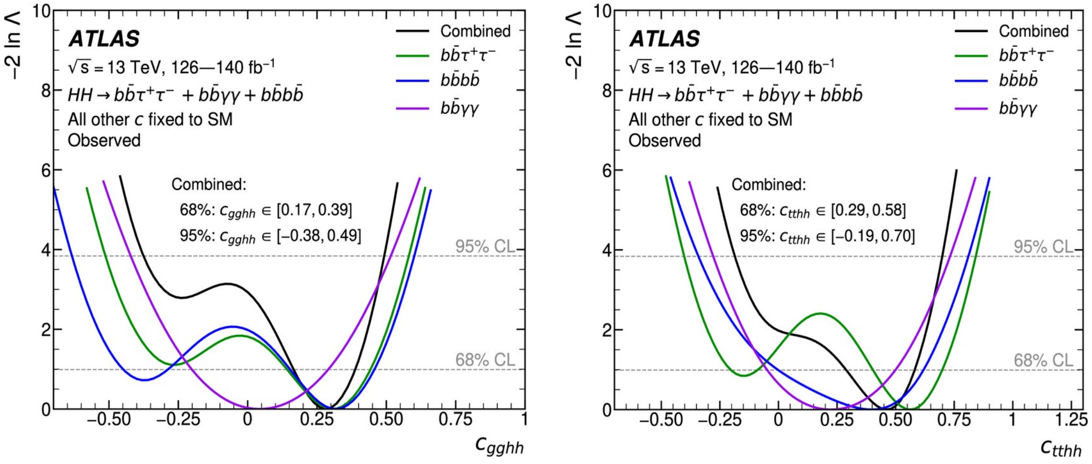

Observed: -0.38< C_{ggHH} < 0.49
Expected: -0.36< C_{ggHH} < 0.36

Observed: -0.19< C_{ttHH} < 0.70
Expected: -0.27< C_{ttHH} < 0.66

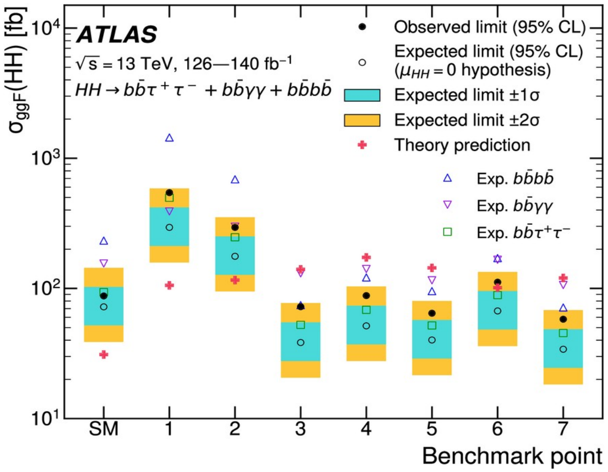

BM3, BM4, BM5, and BM7 scenarios can be excluded

Phys. Rev. Lett. 133 (2024) 101801

Conclusions

- ♦ HH searches are one of the most attractive in particle physics
- ♦ Not offering the unique channel – a combination of searches are necessary
- ♦ HH production provides insight into the Higgs mechanism
- ♦ Good probe for searching processes BSM:
  - Heavy resonance searches
  - DiHiggs production enhancement
- ♦ HEFT four benchmark scenarios excluded
- ♦ New interesting results covering all/partial data collected during LHC RUN3 in the near future...

Thank you

Backup

HH+H Combination

The κ_λ can be measured through loop correction in single Higgs boson production.
By combining HH and H searches additional constraints can by achieved.
Offers most stringent constraint on κ_λ to date.

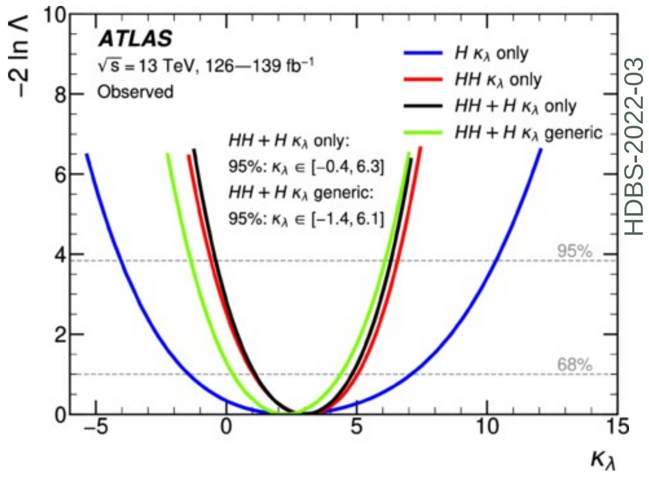

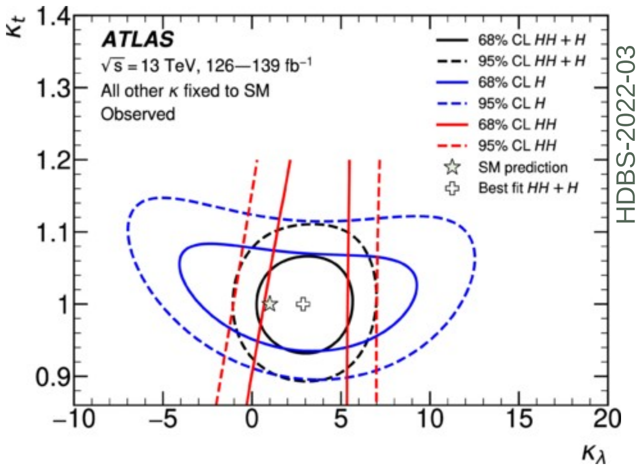

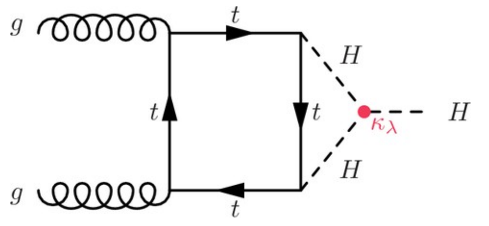

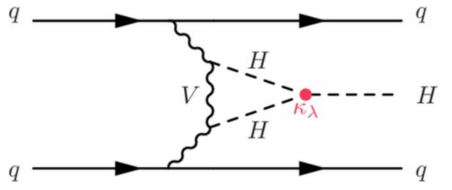

Single H processes:
$H\rightarrow\gamma\gamma$, $H\rightarrow\tau\tau$, $H\rightarrow bb(VH)$,
$H\rightarrow bb(VBF)$, $H\rightarrow bb(ttH)$,
H->ZZ->4l

Observed: $-0.4 < \kappa_\lambda < 6.3$
Expected: $-1.9 < \kappa_\lambda < 7.6$

κ_{2V} =1 for single Higgs, no complete parametrization NLO EW corrections

arXiv:2211.01216v1

HL-LHC prospects

HL-LHC energy $\sqrt{s}$ =14 TeV
HH $\sigma^{SM}_{ggF} = 36.7^{+6\%}_{-23\%}$
HH $\sigma^{SM}_{VBF} = 2.1^{+0.03\%}_{-0.04\%}$
Expected integrated luminosity 3000 fb^{-1}

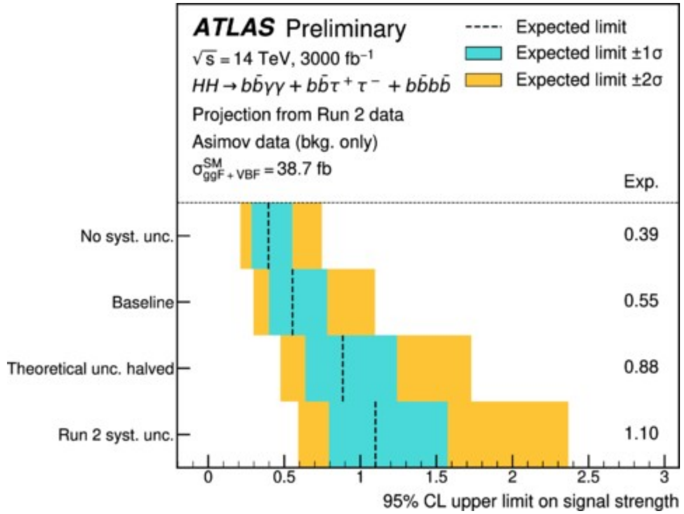

ATL-PHYS-PUB-2022-053

Run 2 distribution scaled by factor 1.18 and 1.19 for ggF and VBF HH signals respectively

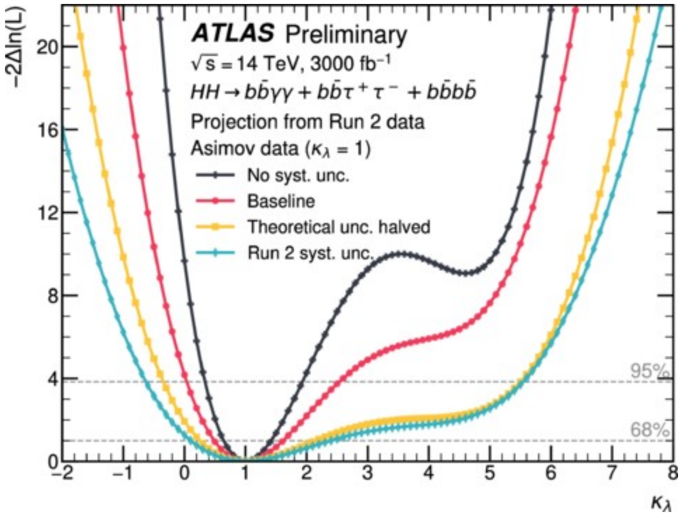

ATL-PHYS-PUB-2022-053

Expected significance (σ) for baseline scenario is 3.4 and observation is expected while 0 > K_λ or K_λ > 5.8

ATL-PHYS-PUB-2022-053

The ATLAS detector

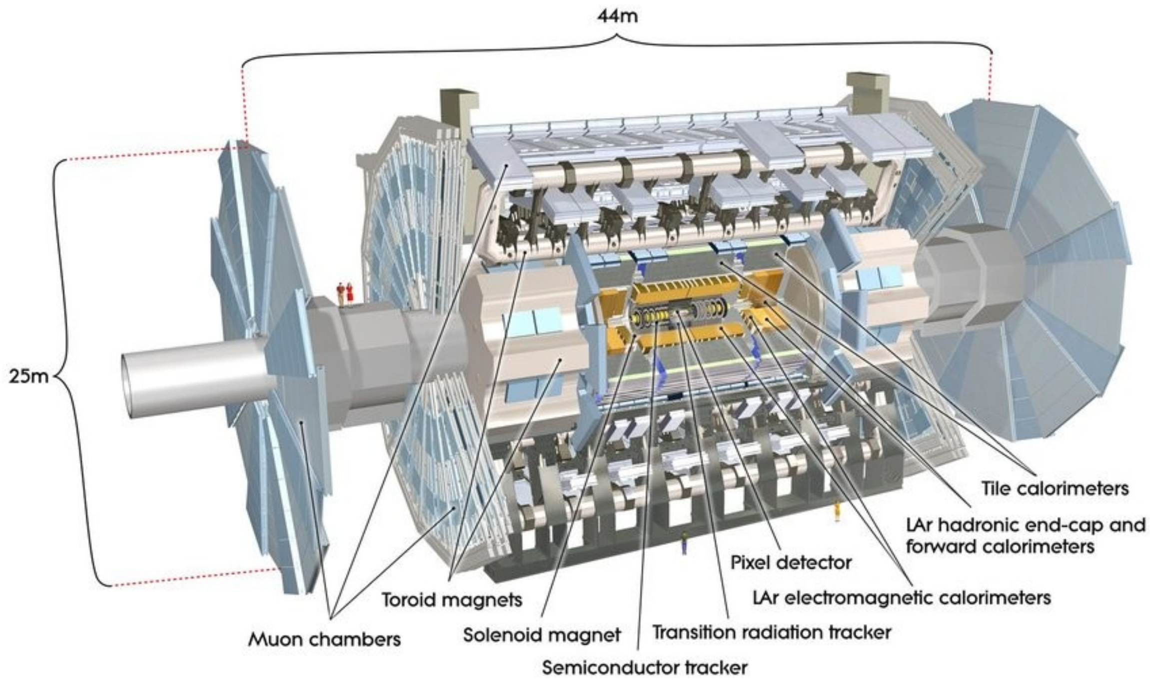

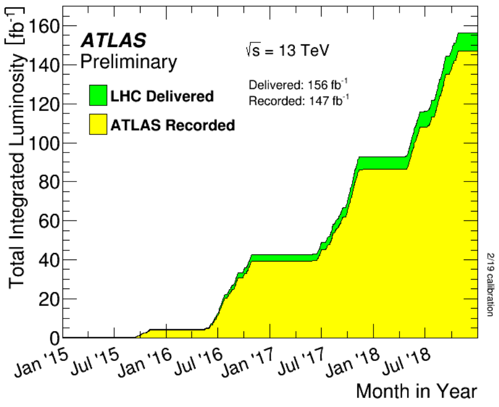

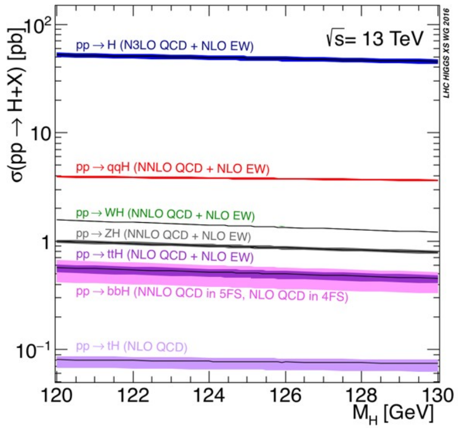

EFT

Standard Model EFT (SMEFT)

► Includes higher-dimensional operators that capture unknown effects, beyond current measurement ability.

► Assumes linear electroweak symmetry breaking (EWSB) with Higgs as the part of doublet

► Probes for the physics beyond SM (heavy resonances,gauge boson interactions, or deviations in Higgs.

Wilson coefficients:
$C_H \sim \kappa_\lambda$, $C_{H\Box}$, C_{HD} , C_{tH}, C_{HG}, C_{tG}

$$\mathscr{L}_{\text{SMEFT}} \supset \frac{c_{H\Box}}{\Lambda^2}(\phi^\dagger\phi)\Box(\phi^\dagger\phi) + \frac{c_{HD}}{\Lambda^2}(\phi^\dagger D_\mu \phi)^*(\phi^\dagger D^\mu \phi) + \frac{c_H}{\Lambda^2}(\phi^\dagger\phi)^3$$
$$+(\frac{c_{tH}}{\Lambda^2}\phi^\dagger\phi\bar{q}_L\tilde{\phi}t_R + \text{h.c.}) + \frac{c_{HG}}{\Lambda^2}\phi^\dagger\phi G^a_{\mu\nu}G^{\mu\nu,a}$$
$$+\frac{c_{tG}}{\Lambda^2}(\bar{q}_L\sigma^{\mu\nu}T^aG^a_{\mu\nu}\tilde{\phi}t_R + \text{h.c.}).$$

Combination

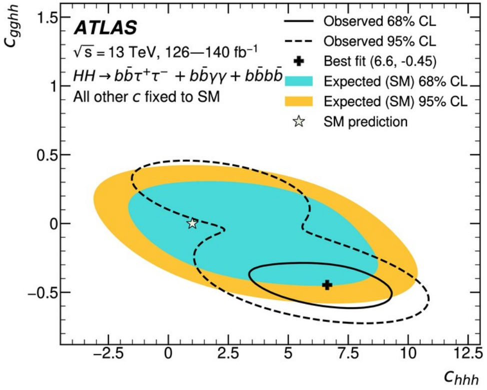

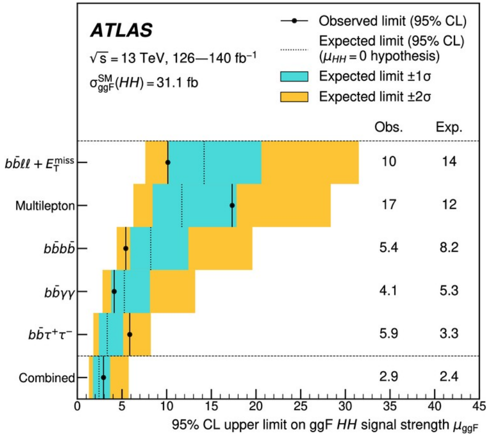

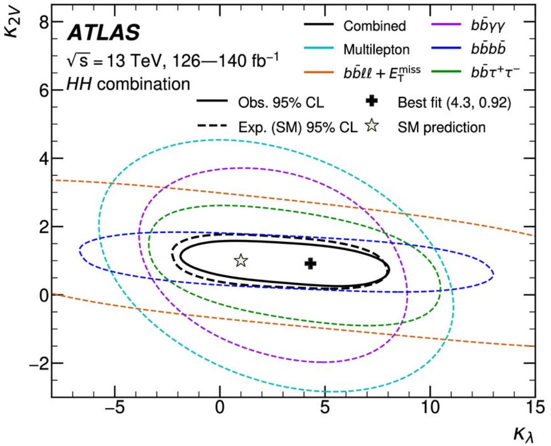

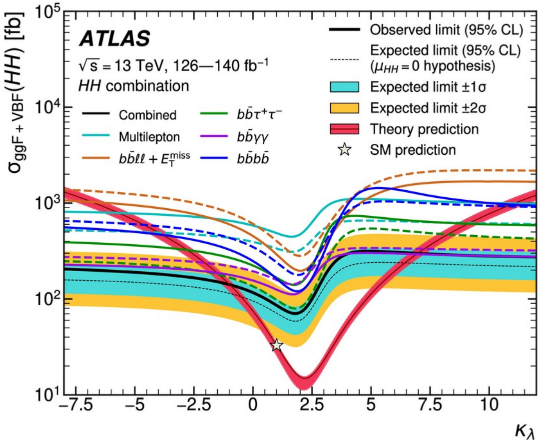

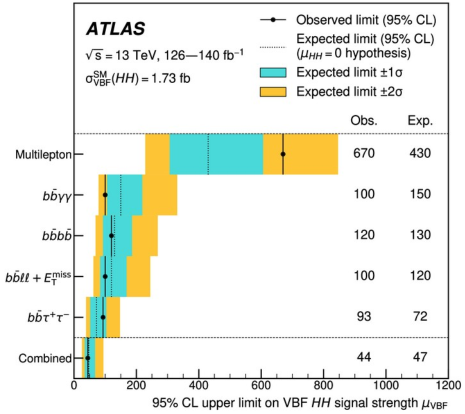

cross-sections

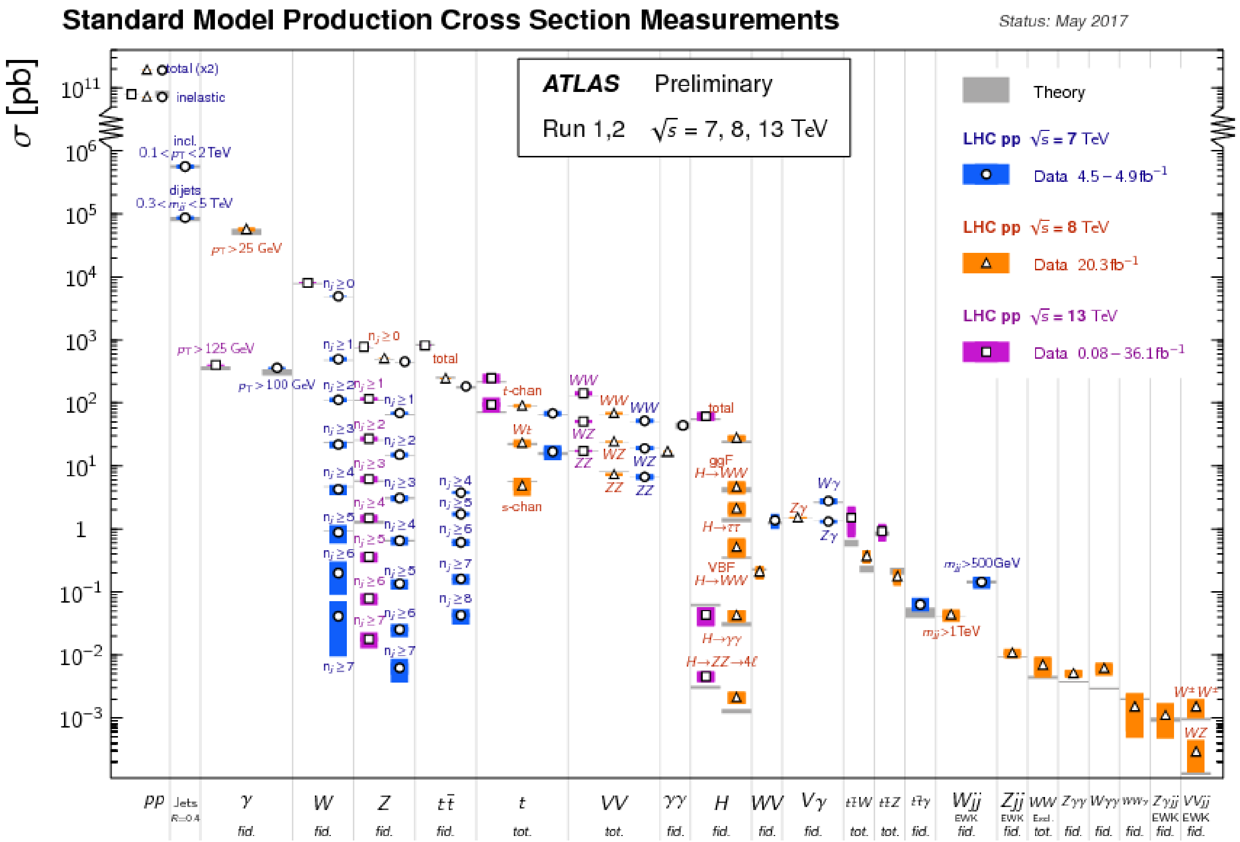

HH → 4b

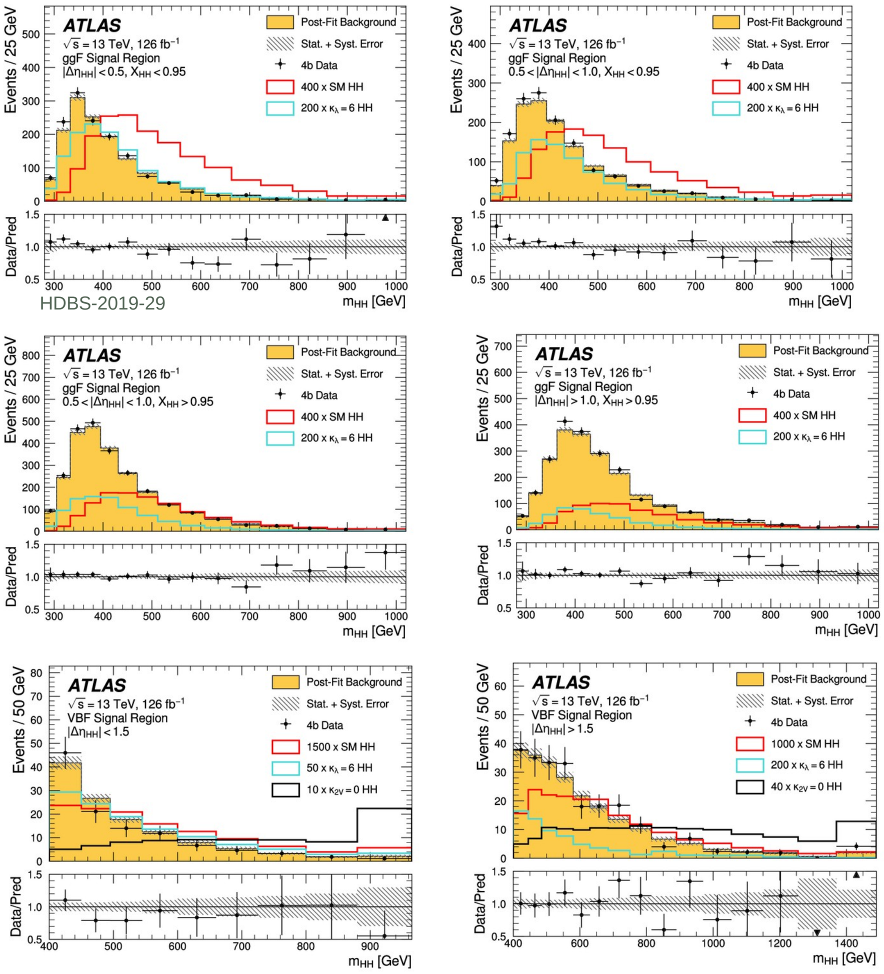

HDBS-2019-29

Source of Uncertainty	$\Delta\mu/\mu$
Theory uncertainties	
Theory uncertainty in signal cross-section	−9.0%
All other theory uncertainties	−1.4%
Background modeling uncertainties	
Bootstrap uncertainty	−7.1%
CR to SR extrapolation uncertainty	−7.5%
3b1f nonclosure uncertainty	−2.0%

$$X_{HH}=\sqrt{\left(\frac{m_{H1}-124\,GeV}{0.1\,m_{H1}}\right)^2+\left(\frac{m_{H2}-117\,GeV}{0.1\,m_{H2}}\right)^2}$$

$$X_{Wt}=min\left[\sqrt{\left(\frac{m_{jj}-m_W}{0.1\,m_{jj}}\right)^2+\left(\frac{m_{jjb}-m_t}{0.1\,m_{jjb}}\right)^2}\right]$$

Effective Filed Theory coefficient results

SMEFT

HDBS-2019-29

Parameter	Expected Constraint		Observed Constraint	
	Lower	Upper	Lower	Upper
c_H	−20	11	−22	11
c_{HG}	−0.056	0.049	−0.067	0.060
$c_{H\Box}$	−9.3	13.9	−8.9	14.5
c_{tH}	−10.0	6.4	−10.7	6.2
c_{tG}	−0.97	0.94	−1.12	1.15

Upper and lower limits on the parameters

HEFT

HDBS-2019-29

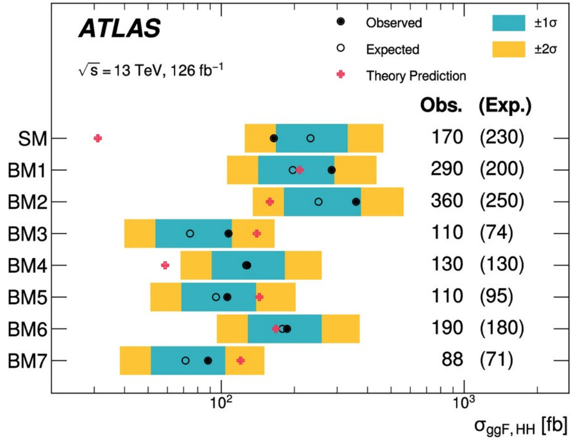

BM3,BM5, and BM7 scenarios can be excluded

Observed: -0.36< C_{ggHH} < 0.78
Expected: -0.42< C_{ggHH} < 0.75

Observed: -0.55< C_{ttHH} < 0.51
Expected: -0.46< C_{ttHH} < 0.4

PHYSICAL REVIEW D 108, 052003 (2023)

$HH \rightarrow 4b$

arXiv:2301.03212

	Observed Limit	-2σ	-1σ	Expected Limit	$+1\sigma$	$+2\sigma$
μ_{ggF}	5.5	4.4	5.9	8.2	12.4	19.6
μ_{VBF}	130	70	100	130	190	280
$\mu_{\text{ggF+VBF}}$	5.4	4.3	5.8	8.1	12.2	19.1

The observed and expected upper limits on the SM ggF HH production cross-section σggF, SM VBF HH production cross-section σVBF, and combined SM ggF and VBF HH production cross-section σggF+VBF at the 95% CL, expressed as multiples of the corresponding SM cross-sections. The expected values are shown with corresponding one- and two-standard-deviation error bounds, and they are obtained using a background-only fit to the data. When extracting the limits on σggF+VBF, the relative contributions of ggF and VBF production to the total cross-section are fixed to the SM prediction.

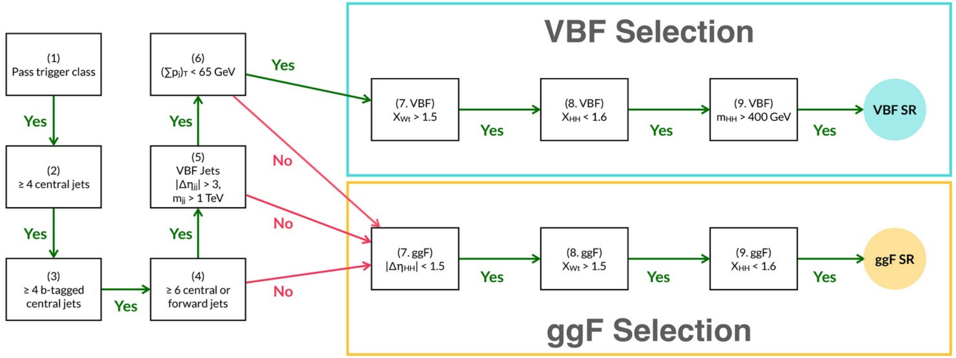

A flowchart summarizing the nine selection criteria used for the VBF and ggF analysis selections. Events must satisfy selection criteria 1-3 in order to be considered for either analysis signal region. Events failing to satisfy any of the selection criteria 4-6 are considered for inclusion in the ggF signal region, while those satisfying selection criteria 4-6 are considered for the VBF signal region.

Parameter	Expected Constraint		Observed Constraint	
	Lower	Upper	Lower	Upper
c_H	−20	11	−22	11
c_{HG}	−0.056	0.049	−0.067	0.060
$c_{H\Box}$	−9.3	13.9	−8.9	14.5
c_{tH}	−10.0	6.4	−10.7	6.2
c_{tG}	−0.97	0.94	−1.12	1.15

The extracted upper and lower limits on the SMEFT parameters to which the analysis is sensitive. For each parameter, the constraints are provided assuming the other parameters are fixed to 0. The VBF HH process is ignored for this result.

HL-LHC prospects

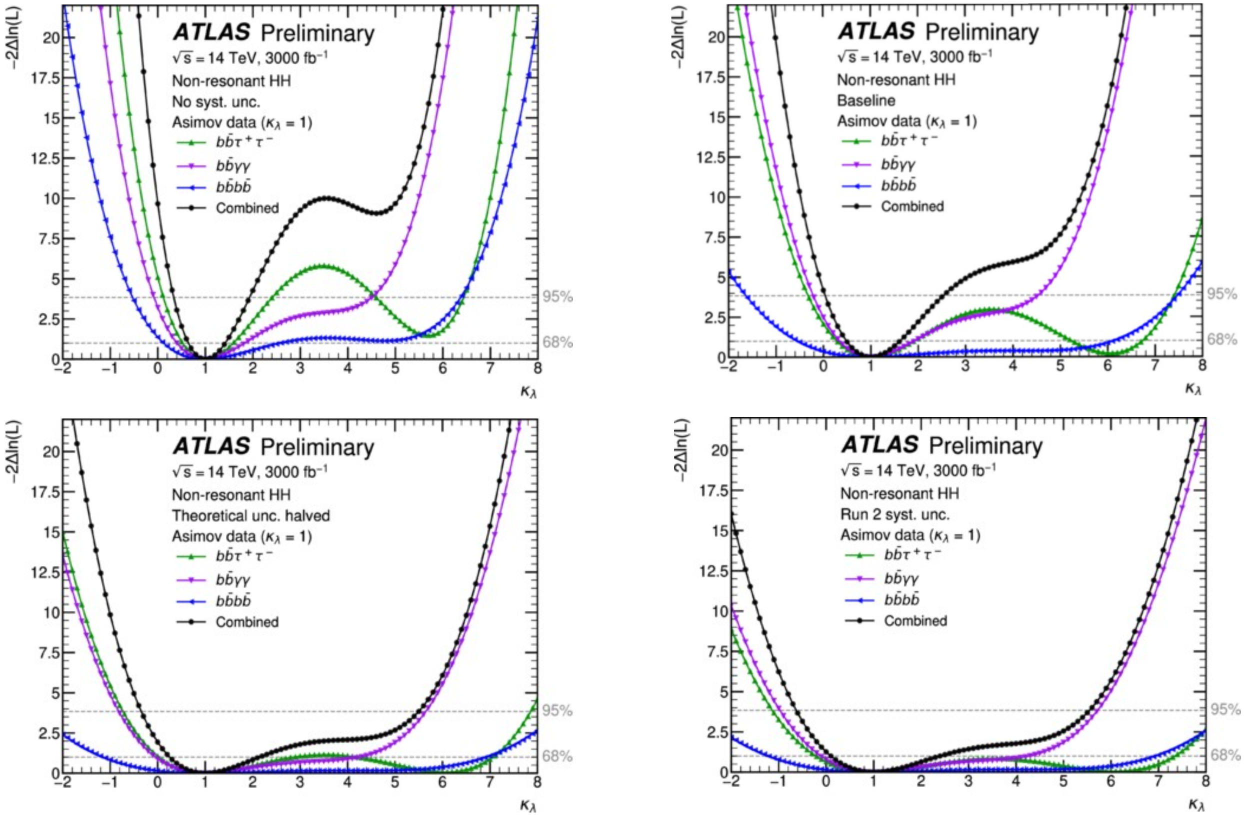

Negative log-profile-likelihood as a function of κλ evaluated on an Asimov dataset constructed under the SM hypothesis of κλ=1, for bb̄γγ, bb̄τ+τ- and bb̄bb̄ projections, and their combination assuming the four different uncertainty scenarios described in the text. The intersections of the dashed horizontal lines with the profile likelihood curve define the 68% and 95% confidence intervals, respectively.

HL-LHC prospects

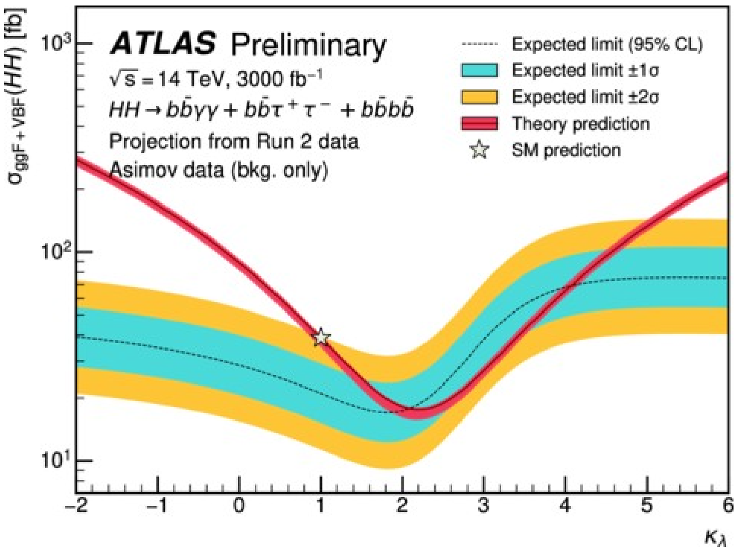

Expected 95% CL limits on the HH cross-section for different κλ hypotheses at √s = 14 TeV, 3000 fb-1 at the HL-LHC with the baseline uncertainty scenario for combination with bb̄γγ and bb̄τ+τ- channels. The expected cross-section limits assume a complete absence of HH production. The theory prediction curve represents the situation where all parameters and couplings are set to their SM values except for κλ. The SM hypothesis corresponds to κλ=1.

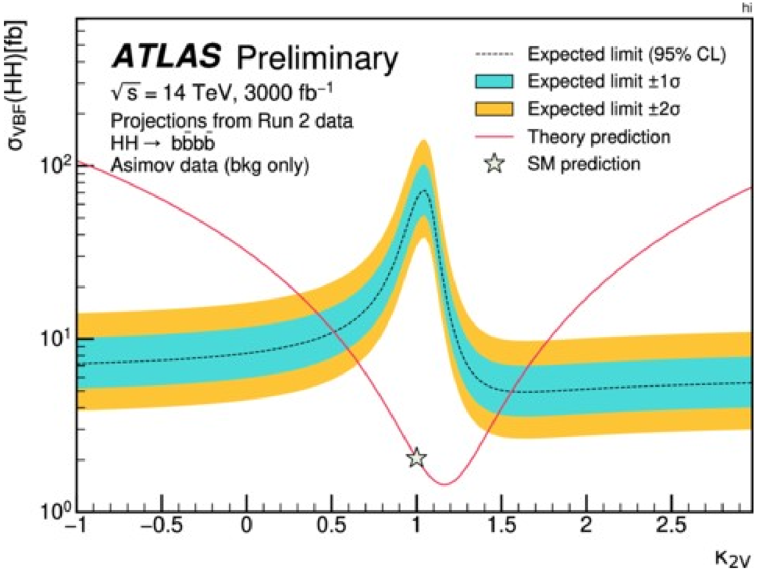

Expected 95% CL limits on the HH cross-section for different κ2V hypotheses at √s = 14 TeV, 3000 fb-1 at the HL-LHC with the baseline uncertainty scenario. The expected cross-section limits assume a complete absence of HH production. The theory prediction curve represents the situation where all parameters and couplings are set to their SM values except for κ2V. The SM hypothesis corresponds to κ2V=1.

HH → bbττ

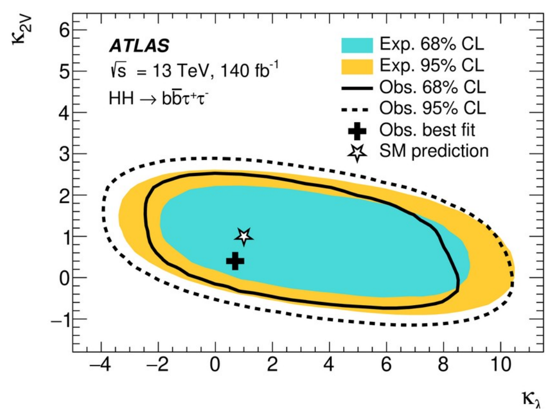

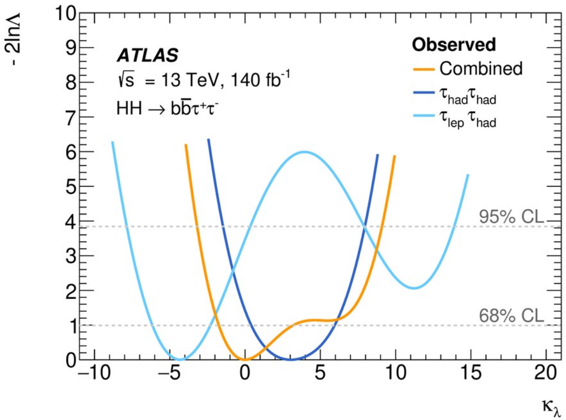

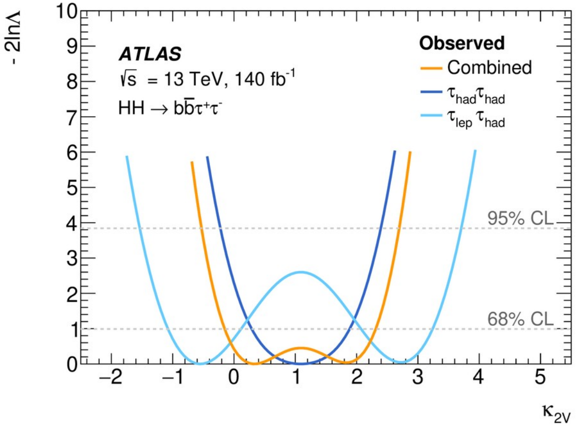

	Acceptance × Efficiency [%]			
	$\tau_{had}\tau_{had}$	$\tau_{lep}\tau_{had}$ SLT	$\tau_{lep}\tau_{had}$ LTT	Total
SM	4.1%	4.1%	1.0%	4.6%
BM 1	1.6%	2.3%	0.6%	2.3%
BM 2	2.3%	2.7%	0.7%	3.0%
BM 3	5.2%	5.1%	0.9%	5.6%
BM 4	4.7%	4.6%	0.9%	5.1%
BM 5	5.6%	5.3%	1.0%	6.0%
BM 6	4.0%	4.1%	0.9%	4.5%
BM 7	6.1%	5.7%	1.0%	6.4%

Wilson coefficient	Observed 95% CI	Expected 95% CI
c_{gghh}	[−0.51, 0.58]	[−0.42, 0.44]
c_{tthh}	[−0.40, 0.84]	[−0.32, 0.72]
c_H	[−19.4, 10.0]	[−19.1, 8.6]
$c_{H\Box}$	[−12.6, 11.6]	[−8.5, 11.1]

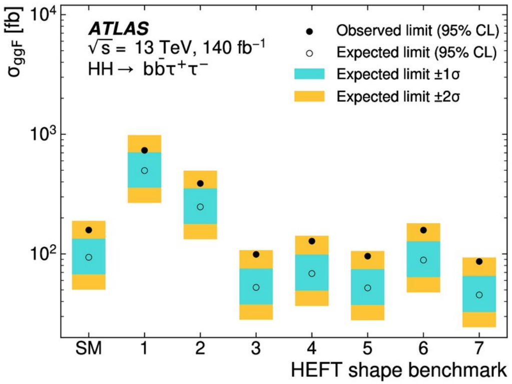

HDBS-2019-27

HH → bbττ

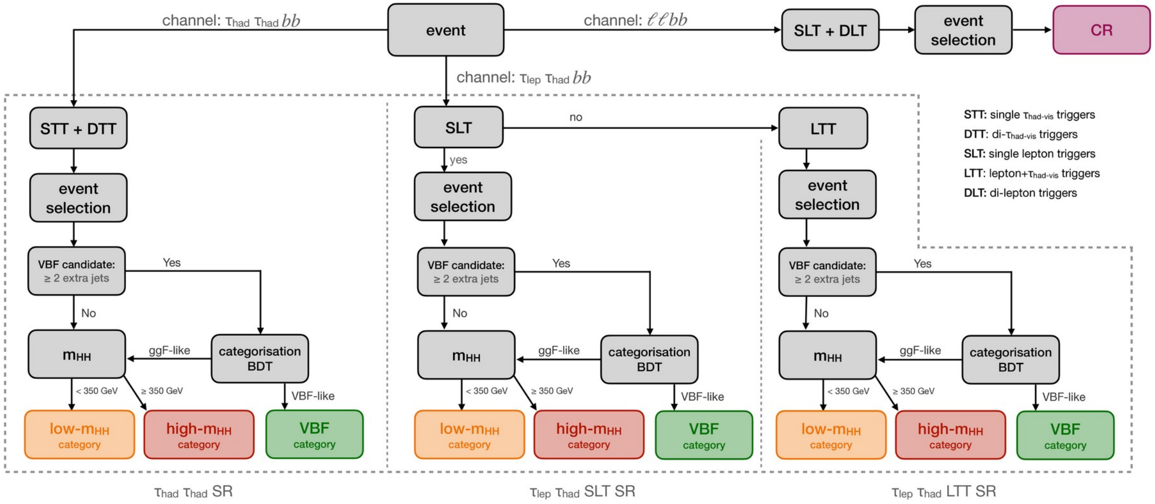

channel: τhad τhad bb
event
channel: ℓℓbb
SLT + DLT
event selection
CR
channel: τlep τhad bb
STT + DTT
SLT
no
LTT
yes
event selection
event selection
event selection
STT: single τhad-vis triggers
DTT: di-τhad-vis triggers
SLT: single lepton triggers
LTT: lepton+τhad-vis triggers
DLT: di-lepton triggers
VBF candidate: ≥ 2 extra jets
Yes
No
mHH
ggF-like
categorisation BDT
< 350 GeV
≥ 350 GeV
VBF-like
low-mHH category
high-mHH category
VBF category
τhad τhad SR
τlep τhad SLT SR
τlep τhad LTT SR

HH → bbττ

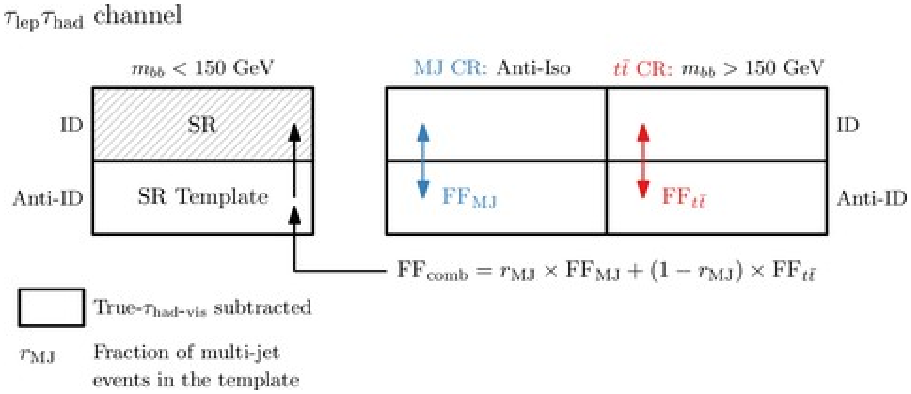

Schematic depiction of the combined fake-factor method used to estimate multi-jet and tt̄ backgrounds with fake-τhad-vis in the τlepτhad channel. Backgrounds which are not from events with fake-τhad-vis originating from jets are estimated from simulation and are subtracted from data in all control regions. Events in which an electron or a muon is misidentified as a τhad-vis are also subtracted, but their contribution is very small. Both sources are indicated by `True-τhad-vis subtracted' in the legend.

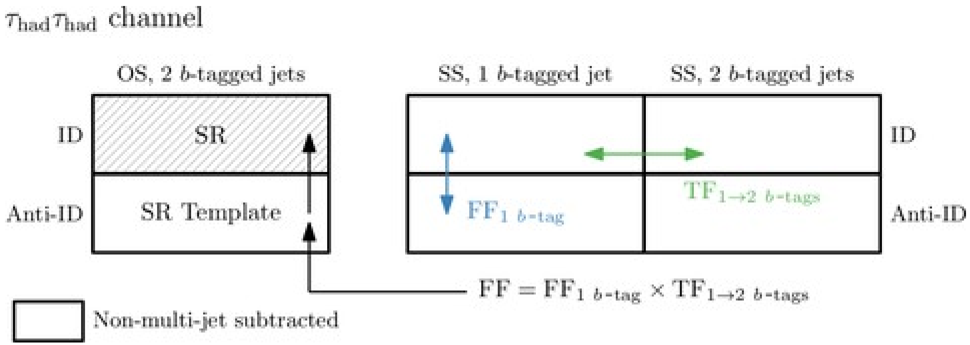

Schematic depiction of the fake-factor method to estimate the multi-jet background with fake-τhad-vis in the τhadτhad channel. Backgrounds that are not from multi-jet events are simulated and subtracted from data in all the control regions. This is indicated by `Non-multi-jet subtracted' in the legend.

τhadτhad		τlepτhad	
STTs	DTTs	SLTs	FTTs
No e/μ Two loose τhad-vis		p_T^e> 25,27GeV p_T^μ> 21,27GeV	18GeV< p_T^e < SLTs 15GeV < p_T^μ < SLTs
p_T > 100,140, 180 (25) GeV	p_T >40 (30)GeV	one loose τhad-vis P_T > 30 GeV	

HH → bbττ

Effective Filed Theory coefficient results

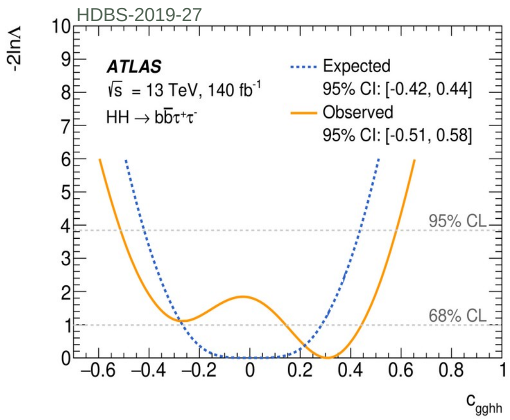

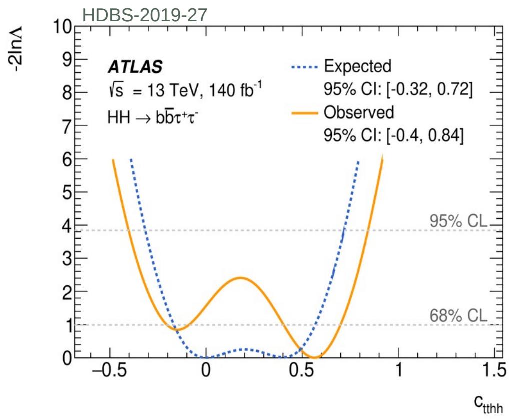

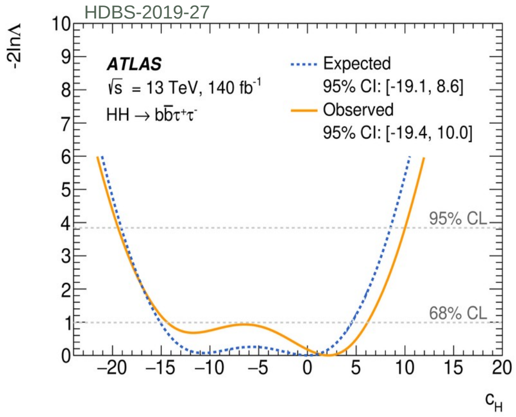

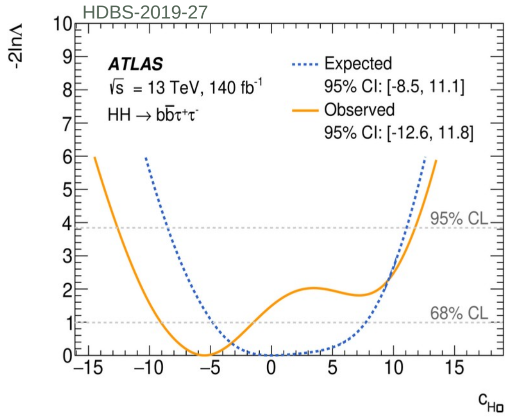

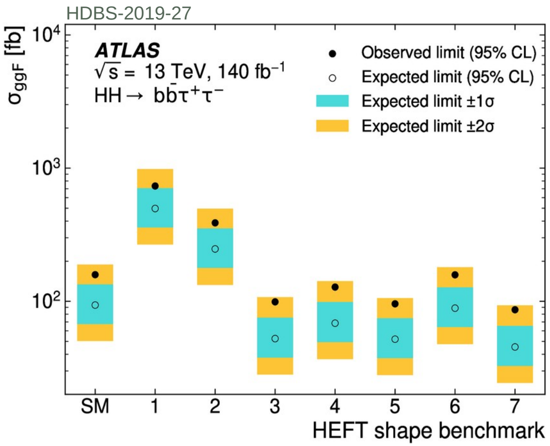

PHYS. REV. D 110, 032012 (2024)

Wilson coefficient	Observed 95% CI	Expected 95% CI
c_{gghh}	[−0.51, 0.58]	[−0.42, 0.44]
c_{tthh}	[−0.40, 0.84]	[−0.32, 0.72]
c_{H}	[−19.4, 10.0]	[−19.1, 8.6]
$c_{H\square}$	[−12.6, 11.6]	[−8.5, 11.1]

Observed and expected 95% CIs on HEFT and SMEFT Wilson coefficients

HH → bbγγ

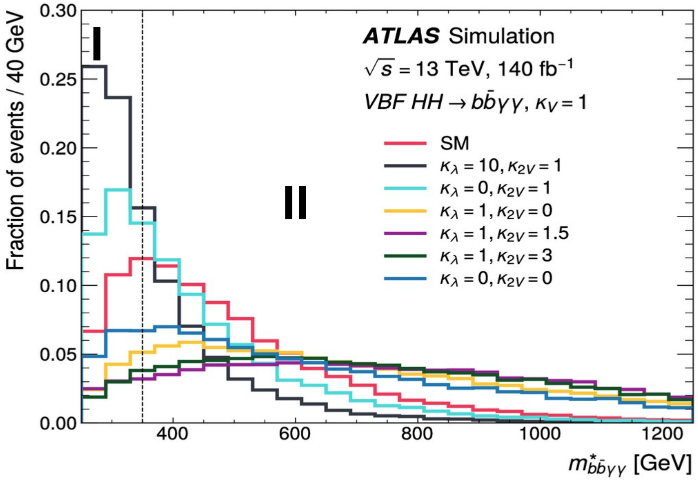

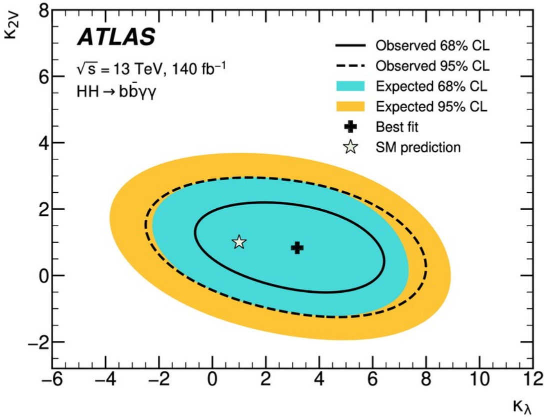

Systematic uncertainty source	Relative impact [%]
Experimental	
Photon energy resolution	0.4
Photon energy scale	0.1
Flavour tagging	0.1
Theoretical	
Factorisation and renormalisation scale	4.8
$\mathcal{B}(H \to \gamma\gamma, b\bar{b})$	0.2
Parton showering model	0.2
Heavy-flavour content	0.1
Background model (spurious signal)	0.1

2 regions for increase sensitivity to:
- **I** – large kλ, BSM, (low masses)
- **II** – small kλ, SM, (high masses)

Category	Selection criteria
High Mass 1	$m^*_{b\bar{b}\gamma\gamma} \geq 350$ GeV, BDT score $\in [0.545, 0.830]$
High Mass 2	$m^*_{b\bar{b}\gamma\gamma} \geq 350$ GeV, BDT score $\in [0.830, 0.905]$
High Mass 3	$m^*_{b\bar{b}\gamma\gamma} \geq 350$ GeV, BDT score $\in [0.905, 1.000]$
Low Mass 1	$m^*_{b\bar{b}\gamma\gamma} < 350$ GeV, BDT score $\in [0.430, 0.785]$
Low Mass 2	$m^*_{b\bar{b}\gamma\gamma} < 350$ GeV, BDT score $\in [0.785, 0.890]$
Low Mass 3	$m^*_{b\bar{b}\gamma\gamma} < 350$ GeV, BDT score $\in [0.890, 0.950]$
Low Mass 4	$m^*_{b\bar{b}\gamma\gamma} < 350$ GeV, BDT score $\in [0.950, 1.000]$

HH → bbγγ

Effective Filed Theory coefficient results

HDBS-2021-10

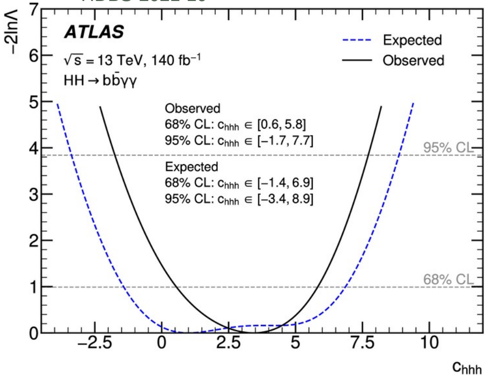

HDBS-2021-10

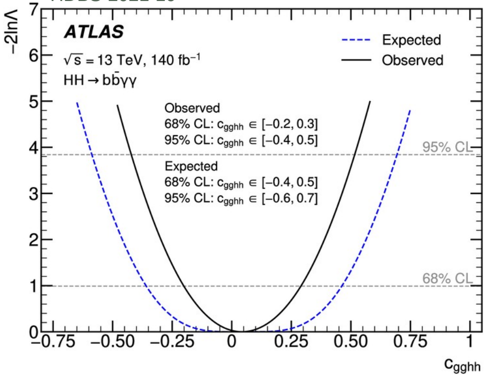

HDBS-2021-10

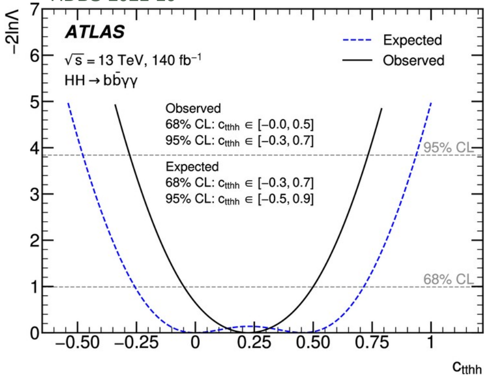

HDBS-2021-10

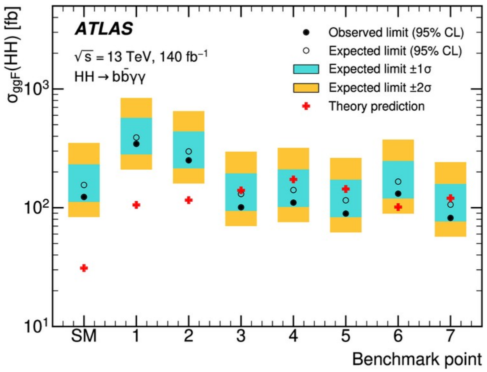

HDBS-2021-10

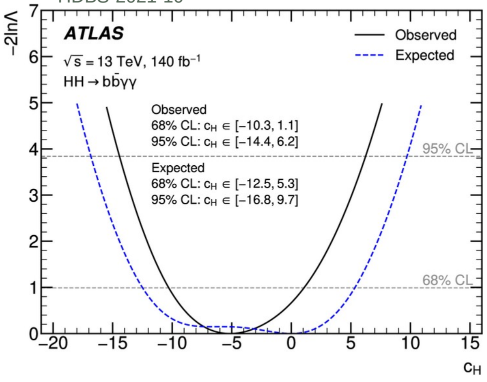

HDBS-2021-10

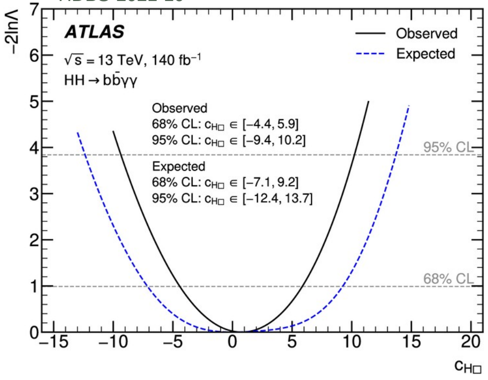

Benchmark	c_{hhh}	c_{tth}	c_{ggh}	c_{gghh}	c_{tthh}
SM	1.00	1.00	0	0	0
1	5.11	1.10	0	0	0
2	6.84	1.03	−1/3	0	1/6
3	2.21	1.05	1/2	1/2	−1/3
4	2.79	0.90	−1/3	−1/2	−1/6
5	3.95	1.17	1/6	−1/2	−1/3
6	−0.68	0.90	1/2	1/4	−1/6
7	−0.10	0.94	1/6	−1/6	1

Wilson coefficient	95% CL Observed	95% CL Expected
c_{hhh}	[−1.7 , 7.7]	[−3.4 , 8.9]
c_{tthh}	[−0.28, 0.73]	[−0.48, 0.94]
c_{gghh}	[−0.42, 0.52]	[−0.59, 0.69]

-14.4 (-16.8) < c_H < 6.2 (9.7) obs.(exp.)

-9.4 (12.4) < $c_{H□}$ < 10.2 (13.7) obs.(exp.)

J. High Energ. Phys. 2024, 66 (2024)